Princeton Plasma Physics Laboratory

PPPL- 4474

PPPL- 4474

Intra-shot MSE Calibration Technique For LHCD Experiments

Jinseok Ko, Steve Scott, Syun'ichi Shiraiwa, Martin Greenwald,
Ronald Parker, and Gregory Wallace

November, 2009

Prepared for the U.S. Department of Energy under Contract DE-AC02-09CH11466.

Princeton Plasma Physics Laboratory
Report Disclaimers

Full Legal Disclaimer

Trademark Disclaimer

PPPL Report Availability

Princeton Plasma Physics Laboratory:

http://www.pppl.gov/techreports.cfm

Office of Scientific and Technical Information (OSTI):

http://www.osti.gov/bridge

Related Links:

U.S. Department of Energy

Office of Scientific and Technical Information

Fusion Links

Intra-shot MSE calibration technique for LHCD experiments

Jinseok Ko,[1] Steve Scott,[2] Syun'ichi Shiraiwa,[3] Martin Greenwald,[3] Ronald Parker,[3] and Gregory Wallace[3]
[1)] *MIT Plasma Science and Fusion Center, Cambridge, Massachusetts*[a)]
[2)] *Princeton Plasma Physics Laboratory, Princeton, New Jersey*
[3)] *MIT Plasma Science and Fusion Center, Cambridge, Massachusetts*

(Dated: 23 November 2009)

The spurious drift in pitch angle of order several degrees measured by the Motional Stark Effect (MSE) diagnostic in the Alcator C-Mod tokamak[1] over the course of an experimental run day has precluded direct utilization of independent absolute calibrations. Recently, the underlying cause of the drift has been identified as thermal stress-induced birefringence in a set of in-vessel lenses. The shot-to-shot drift can be avoided by using MSE to measure only the change in pitch angle between a reference phase and a phase of physical interest within a single plasma discharge. This intra-shot calibration technique has been applied to the Lower Hybrid Current Drive (LHCD) experiments and the measured current profiles qualitatively demonstrate several predictions of LHCD theory such as an inverse dependence of current drive efficiency on the parallel refractive index and the presence of off-axis current drive.

I. INTRODUCTION

Information on the internal profiles of local current density and safety factor is typically provided by MSE diagnostics[2]. The MSE diagnostic on the Alcator C-Mod tokamak[3–5] is a conventional MSE system based on the original PBX-M design[2]. A 10-cm diameter, 50 keV neutral hydrogen beam is injected into the C-Mod torus along the horizontal midplane, approximately 7^o off-normal. Beam neutrals are promoted into various excited states through collisions with the plasma ions and electrons and emit a spectrum that is Doppler-shifted due to the beam motion, and Stark-split due to the large motional electric field experienced by the beam neutrals in their reference frame. The emission lines are linearly polarized either parallel (σ lines) or perpendicular (π lines) to the local magnetic field (σ lines). This light is collected by an in-vessel, polarization-preserving optical system, shown in Figure 1, and is then conveyed via an optical train to two ex-vessel photoelastic modulators (PEM's) and a linear polarizer that encode the polarization direction as intensity modulations at twice the frequencies of the PEM's. The modulated light is carried ∼20 m by fiber optic to a remote diagnostic suite where it passes through temperature-controlled narrow passband ($\Delta\lambda \sim$ 1 nm) interference filters that select wavelengths exclusively from the Balmer-series π lines. Finally, the light intensity is measured by avalanche photodiodes and is digitized at 1 MHz for off-line analysis.

A complex in-vessel optical train consisting of five lenses (one singlet and two doublets) and three flat dielectric mirrors is utilized on C-Mod to capture light emitted by the DNB, reflect it twice through $\sim 90^o$, and convey it through a vacuum window directly above the DNB and then onward through an ex-vessel linear optical train that includes the PEM's. The in-vessel optical components are housed in a stainless steel periscope. The system supports ten spatial channels that view the DNB from $r/a \approx 0.1-0.9$ with modest spatial resolution, $\Delta r/a = 0.09$ at the plasma edge and 0.41 at the center.

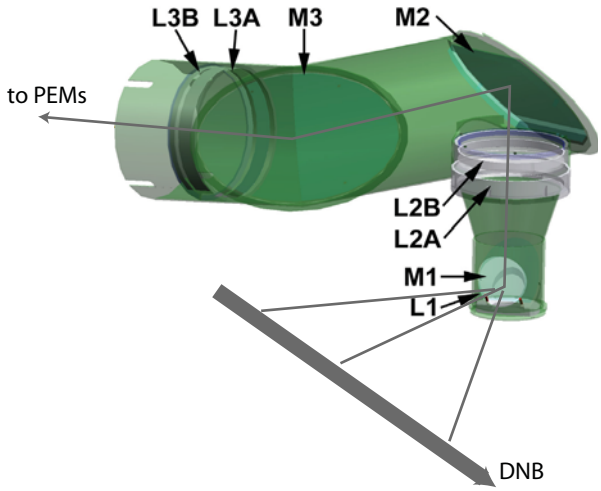

FIG. 1. Three dimensional view of the invessel MSE periscope. Light passes through lens L1, through lens pair L2(A,B), through lens pair L3(A,B) and is reflected off mirrors M1, M2, and M3.

For several years, the MSE system on C-Mod has experienced large, spurious drifts of order several degrees in measured pitch angle over the course of a run day[6] which has precluded direct measurement of the current density profile. Recent experiments have traced this difficulty to thermal stress-induced birefringence on a lens doublet within the in-vessel optical system. Details of the thermal birefringence problems are introduced in Section II. The time scale for thermal birefringence to alter MSE's performance is shown to be long compared to a single plasma discharge, which motivates the use of an 'intra-shot' calibration technique that effectively uses MSE only to measure *changes* in the pitch angle profile

[a)] Current affiliation: University of Wisconsin, Madison, Wisconsin

during LHCD experiments. This scheme is presented in Section III. Section IV applies this technique to infer the current density in the LHCD experiments and Section V concludes this paper.

II. THERMAL STRESS BIREFRINGENCE

The use of lenses as components of a polarization-preserving optical system inside the dynamic temperature environment of a tokamak has proven to be a major difficulty. The underlying cause of the spurious variability has been identified in a recent series of in-vessel and optical-bench tests[6,7]: thermal stress birefringence on a particular lens doublet ('L2A' and 'L2B' in Figure 1) near the middle of the in-vessel optical train. The bench tests demonstrated that as MSE is illuminated with linearly polarized light of fixed polarization direction, the measured polarization angle changes spuriously by up to 20^o as the periscope housing is locally heated by 50 Celsius with a resistive heating tape. By contrast, the spurious change in polarization angle was $\leq 0.8^o$ as the same temperature slew rate was applied to the plasma-facing lens L1 or to the lens doublet L3. The vastly different response of the MSE diagnostic to heating L2 versus L1 or L3 is understood to be a consequence of the image focus at these locations; light from a particular MSE spatial channel reaches a near-focus at L2 which thereby imposes the same stress-induced retardation on all photons. By contrast, the image for a given spatial channel nearly fills the entire lens cross-section at L1 and L3. It is straightforward to show that imposing a retardation onto linearly polarized light yields elliptically polarized light and a change in the polarization direction[6]. Stress-induced birefringence still imposes a retardation and a change in polarization direction for light passing through a particular spot on the L1 and L3 lenses, but the net effect on the average polarization direction, i.e. integrating over all light incident across the lens, is much reduced. The change in net polarization direction would be identically zero if the stress pattern and the incident light intensity were azimuthally symmetric.

The ambient temperature environment for the MSE in-vessel optics is complicated by the presence of nightly heating cycles (to $\sim$ 90 Celsius) followed by a cooling period of several hours at the start of an experimental run day, interspersed with transient heating by plasmas every $\sim$ 15 minutes. As illustrated in Figure 2, the spurious changes in measured polarization angle are significantly reduced if special care is taken to minimize the usual ambient torus temperature variation. This exercise confirms that temperature variations are the cause of the spurious drift and that reducing the temperature variations will reduce that drift. Various measures to reduce the temperature fluctuation of the in-vessel MSE optics including a radiative thermal shield were implemented prior to the FY2009 Alcator C-Mod run campaign. Details of these activities including the thermal design, the expected reduction in stress in the lenses, and the associated reduction in spurious changes in measured angle are discussed in references[7–9].

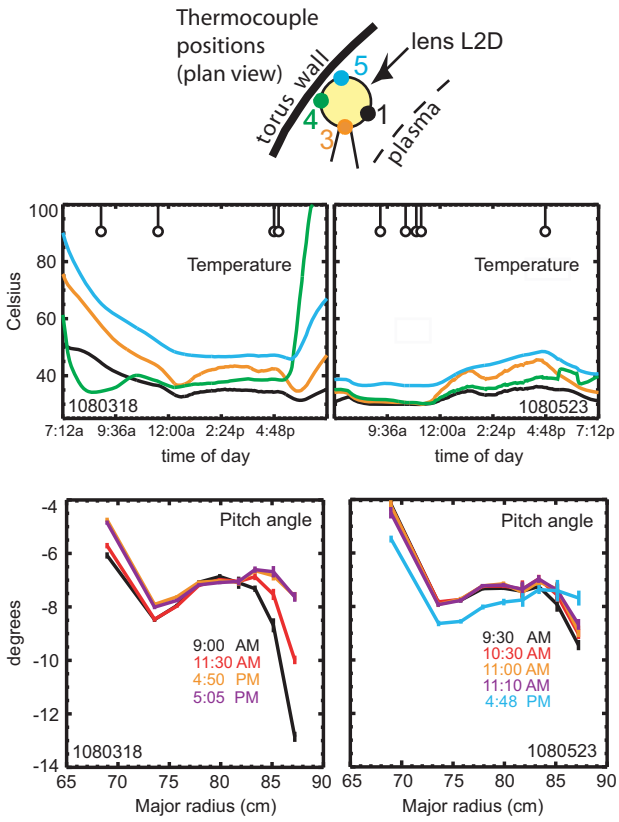

FIG. 2. MSE invessel periscope thermocouple locations, temperature time evolution, and the pitch angle profiles at selected time points from beam-into-gas experiments 1080318 and 1080523. Tick marks in plots of temperature time evolution denote times at which pitch angle profiles were measured. L2D refers to L2A and L2B in Figure 1

.

For the upcoming Alcator C-Mod experimental run campaign and beyond, we expect that the measures taken to reduce the temperature gradients in the in-vessel lenses will reduce the spurious changes in measured polarization angle to negligible levels. This will allow a single calibration of MSE to be accurately applied to an entire multi-month run campaign. The question arises as to whether *existing* MSE measurements can be exploited in any way to yield useful information about behavior of the current density profile – despite the known, large spurious drift due to thermal stress birefringence. This is an important issue because Alcator C-Mod has already carried out a number of current modification experiments using Lower Hybrid Current Drive ([10–12]) during which the MSE diagnostic was functioning.

III. INTRA-SHOT CALIBRATION TECHNIQUE

The crucial circumstance that we exploit is that the spurious drift is apparently caused by thermal stress only in the two in-vessel L2 lenses. Therefore, if over some period of time the temperature profile across the L2 lenses remains constant, then the stress state as well as the spurious change in polarization angle should also remain constant. A calibration of the MSE diagnostic at any time point within this interval should be applicable to all time points within that interval. The L2 lenses are supported by three 1 mm thick Viton O-rings inside a ∼1 cm thick Inconel lens mount. The lens mount is affixed to the inside of the stainless steel periscope housing, approximately 0.16 cm thick. The duration of a typical Alcator C-Mod plasma is ∼2 seconds, which is long compared to the characteristic time for heat to penetrate through the periscope housing (0.25 seconds). Thus, the temperature of the periscope housing can vary significantly during the course of a single plasma discharge, but the characteristic time for heat to be conveyed conductively through the lens mount is ∼14 seconds, and the time for heat to be conveyed through the O-ring is ∼13 seconds. Thus, on the time scale of a single plasma, heat radiated from the plasma to the periscope housing will not change the temperature distribution or the stress distribution in the L2 lenses. Variations in the periscope housing temperature will also be communicated to the lenses through exchange of thermal radiation, but this process is even slower. This suggests that if MSE can be calibrated at one time point during a plasma discharge, then that calibration can be confidently applied to the remainder of the plasma. The basic approach is:

1. Infer a baseline pitch angle profile ($\gamma_0(r)$) from the magnetic reconstruction code EFIT[13–15] at a quiescent Ohmic phase of the shot ($t = t_0$), typically a time point shortly before the start of LHCD These EFIT reconstructions utilize the sawtooth inversion radius measured by Electron Cyclotron Emission (ECE) measurements[16] as an additional constraint: EFIT adjusts the value of the safety factor at the magnetic axis until the reconstructed $q(r)$ profile yields $q = 1$ at the sawtooth inversion radius, following the classical Kadomtsev sawtooth model[17].

2. Use MSE to measure the *change* in pitch angle ($\Delta\gamma(r,t)$) relative to the baseline pitch angle at the quiescent Ohmic phase.

The final inferred pitch angle profile $\gamma(r,t)$ is given by the sum of the baseline profile and the measured pitch angle change,

$$\gamma(r,t) = \gamma_0(r) + \Delta\gamma(r,t) \qquad (1)$$

and is used as a constraint in the final EFIT magnetic reconstruction from which other quantities such as the q-profile and current density profile are computed.

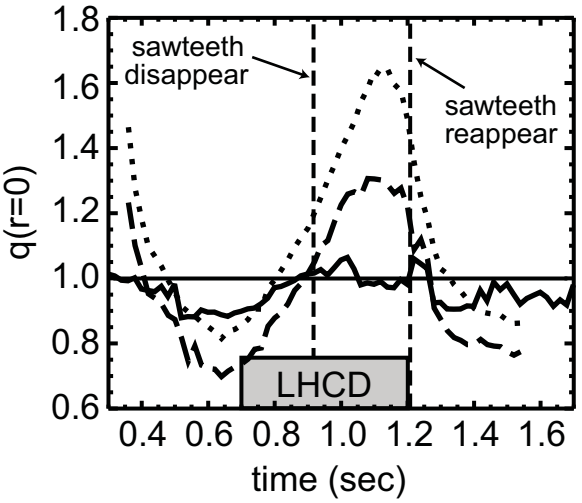

FIG. 3. Time evolution of q_0 calculated by EFIT for plasma 1080320013 with LHCD based on three models. Solid: $q_o \approx 0.95$, without use of MSE's measurement of changes to pitch angle. Dotted: $q_o \approx 0.95$ in the pre-LHCD Ohmic phase, elsewhere using MSE's measurement of changes to the pitch angle profile. Dashed: $q(r = r_{SIR}) \equiv 1.0$ in the Ohmic phase, elsewhere using MSE's measurement of changes to the pitch angle profile. Vertical lines denote the times at which sawteeth disappear and reappear as inferred from ECE measurements.

The timing of disappearance and reappearance of sawteeth as measured by ECE is investigated to check the validity of the intra-shot calibration technique. Figure 3 plots the time history of $q(r = 0)$ as computed by EFIT that was constrained by the pitch angle profile inferred from the intra-shot calibration technique in the usual way, $\gamma(r,t) = \gamma_0(r) + \Delta\gamma_m(r,t)$ (Eq. 1). The evolution of $\gamma(r,t)$ and therefore EFIT's computation of $q(r = 0,t)$ depends on both the accuracy of the pitch angle profile in the Ohmic phase as well as MSE's measurement of the change in pitch angle during and following LHCD. From Figure 3 (*dashed line*) we observe that at the time of disappearance of sawteeth occurs when EFIT computes a value for q_0 of about 1.05. Following the termination of LHCD, the sawteeth reappear when EFIT's value of q_0 is slightly higher, about 1.17.

By comparison, let $\gamma_{AN}(r)$ be the baseline pitch angle profile in the Ohmic phase computed by EFIT without invoking the measured sawtooth inversion radius as a constraint. In this case the value of q_o is regarded by EFIT as a 'measurement' with value 0.95, and EFIT adjusts the computed equilibrium to minimize the least-squares error to this ersatz measurement in addition to the other external magnetic measurements. Then the subsequent pitch angle evolution can be propagated forward using MSE's measurement of the change in pitch angle, $\gamma_1(r,t) = \gamma_{AN}(r) + \Delta\gamma_m(t)$. The time evolution of q_0 computed by EFIT when $\gamma_1(r,t)$ is used as an input to EFIT is illustrated in Figure 3 (*dotted line*). Note that the agreement with respect to timing of the disap-

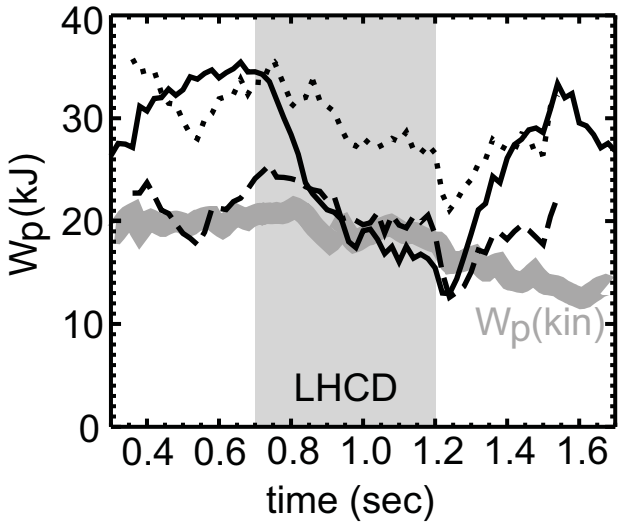

FIG. 4. Comparison of plasma stored energy as measured kinetically (thick gray solid) with EFIT magnetic constructions that (a) assume $q_o \approx 0.95$, unconstrained by MSE pitch angle measurements (Solid); (b) assume $q_o \approx 0.95$ in the Ohmic phase, constrained by MSE measurements of the change in pitch angle (Dotted); and (c) are constrained to match the sawtooth inversion radius in the Ohmic phase, and also constrained by MSE measurements of the change in pitch angle (Dashed).

pearance and reappearance of the sawteeth is less good than if the baseline pitch angle profile is constrained by sawtooth inversion radius. We conclude that, not surprisingly, constraining EFIT with information regarding the the sawtooth inversion radius improves the accuracy of the magnetic reconstruction. Overall, this comparison provides reasonable confirmation of the intra-shot calibration technique given its limitation that the MSE measurement of pitch angles is integrated over 80 milliseconds.

As a second validation of the intra-shot calibration technique, we compare the total stored energy as computed from magnetics (EFIT) with the kinetic stored energy $W_p(kin)$. The electron kinetic energy is obtained from Thomson scattering measurements. The ion temperature profile is computed assuming its shape is the same as that of the electrons, with a magnitude adjusted to match the total neutron emission. The ion density is measured from the effective ion charge, Z_{eff}, assuming the ratio of electron to ion densities is constant across the profiles. Figure 4 illustrates the stored-energy comparison in an LHCD shot. It is shown that the EFIT magnetics reconstruction that does not utilize the MSE measurements of pitch angle (solid) exhibit a significant, spurious decrease (factor 2-3)of stored energy during LHCD that is not reflected in the kinetic measurements. The best agreement with the kinetic stored energy is achieved by the standard intra-shot calibration technique that uses the measured sawtooth inversion radius to constrain the magnetic equilibrium in the baseline Ohmic phase, and MSE to measure changes to the pitch angle profile elsewhere in the plasma. The fact that total stored energy remains relatively constant despite injection of about 0.9 MW of Lower Hybrid power in these plasmas is thought to be a consequence of the associated reduction in Ohmic input power.

IV. APPLICATIONS TO LHCD EXPERIMENTS

The intra-shot calibration technique described above was used to analyze the pitch angle profile for a series of LHCD discharges with the lower hybrid heating power of ≈ 1 MW. The diagnostic neutral beam operated close to its maximum performance, and the plasma density ($\bar{n}_e \approx 5 \sim 7 \times 10^{19} m^{-2}$) was modest relative to typical C-Mod values, ensuring good beam penetration and high signal-to-background for the MSE measurements. For these shots, the plasma current (0.8 MA) and toroidal field (6.2 T) were held constant from 0.5 to 1.5 seconds, while the lower hybrid power was applied from 0.7 to 1.2 seconds. For this analysis, the reference baseline Ohmic phase was taken from 0.55 to 0.65 seconds. Figure 5 compares the radial profile of the toroidal current density (J_ϕ) at the midplane from Ohmic (*top*) and LHCD (*bottom*) phases for four different refractive indices of the LH wave ($n_{||}$). Note, from the left panel in Figure 5, that there was excellent reproducibility in plasma conditions throughout this experiment, as reflected in the relatively small variability in inferred $q(r)$ and $J_\phi(r)$ during the Ohmic pre-LHCD phase. It is evident that as $n_\parallel$ decreases, the on-axis current density is decreased and that the current density off-axis ($r/a \approx 0.8$) increases. The on-axis current density is decreased from 20 to 12 MA/m^2 at $n_{||} = 1.56$.

By subtracting the part of the current density which can be attributed to purely Ohmic induction from the total current density measured by MSE, it is possible to infer the component driven by Lower Hybrid. The total parallel current density in general can be written as, ignoring the bootstrap current,

$$J_{||} = J_{OH} + J_{LH} = \sigma_{neo} E_{||} + J_{LH}, \qquad (2)$$

where J_{OH} is the Ohmic inductive current density, J_{LH} is the current density from LHCD, $E_{||}$ is the parallel electric field, and σ_{neo} is the conductivity which can be scaled with plasma temperature and average ion charge. $E_{||}$ is obtained from the flux-surface-averaged loop voltage inferred from successive EFIT calculations of the poloidal flux function divided by the toroidal circumference of each major radius. It is possible to eliminate the unknown proportionality constant for σ_{neo} using a technique similar to the intra-shot MSE calibration. Finally, using $J_{||}$ obtained from the intra-shot calibration and linearly interpolating Z for the LHCD phase, J_{LH} in Eqn 2 can be inferred. Note that the J_{LH} profile obtained

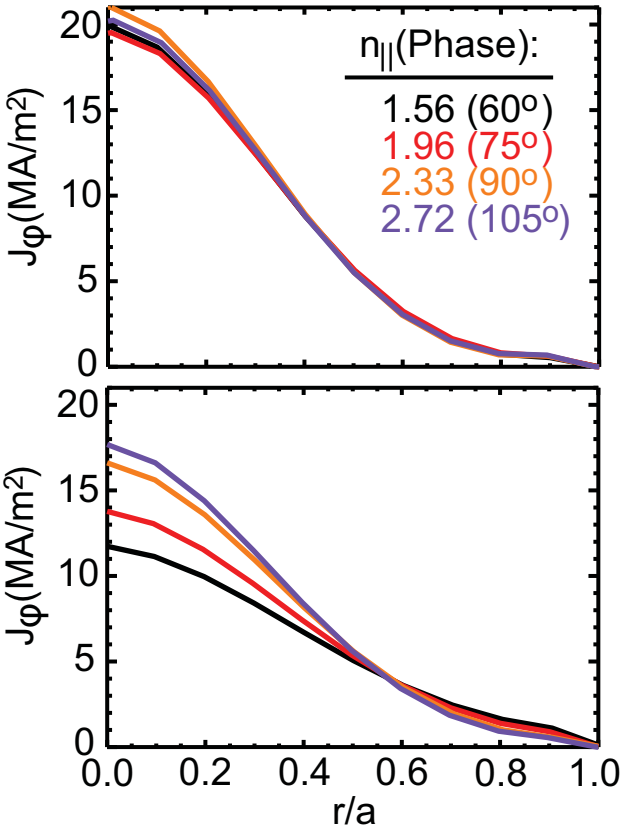

FIG. 5. Radial profiles of toroidal current density (J_ϕ) at the midplane for four groups of shots with different $n_{||}$'s. The plot on the top is from a pre-LHCD phase (Ohmic flattop at t = 0.65 sec) and the plot on the bottom is from a time interval during the LHCD pulse (t = 1.025 sec).

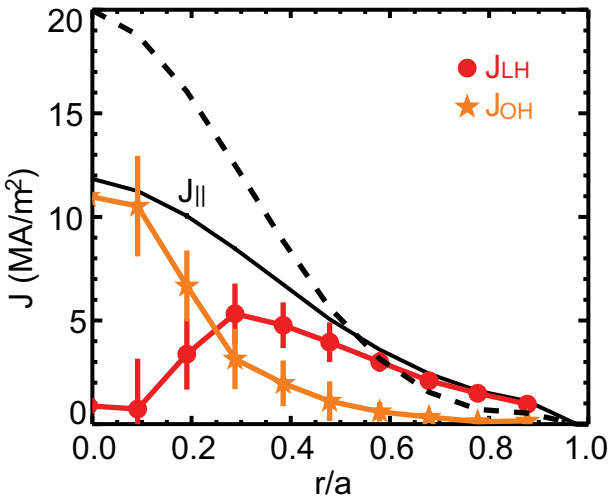

FIG. 6. Radial profiles of current densities in Eqn 2 from Shot 1080320012. The dashed curve represents the profile at the pre-LHCD Ohmic time 't_0' (averaged over 0.6 ∼ 0.65 sec).

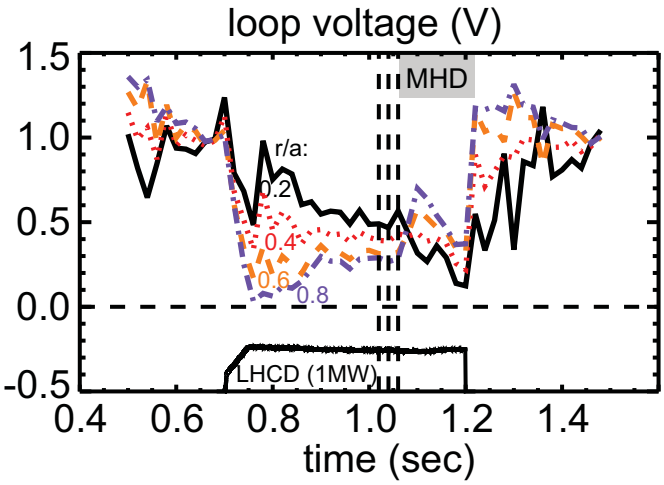

FIG. 7. Time evolution of loop voltage at four radial locations from Shot 1080320012. The vertical lines denote the time points which were averaged to produce the current density profiles shown in Figure 6

through this procedure represents the sum of the current driven directly by Lower Hybrid, plus an *inductive* component which is driven by LH-induced fast electron population responding to $E_{||}$. Also, note that the current densities from the intra-shot calibration method are *local* whereas those in Eqn 2 are *flux-surface-averaged*. Therefore, this analysis is only zeroth-order, probably overestimating the magnitudes due to the inclusion of neoclassical Pfirsch-Schlüter current.

The results of this analysis for shot 1080320012 ($n_{||}$ = 1.56) indicate that the Lower-Hybrid driven current profile peaks off-axis with a broad maximum occurring at approximately $r/a = 0.3$, as illustrated in Figure 6. The measurement uncertainty in J_{LH} and J_{OH} is rather large, mainly due to uncertainties in the loop voltage which is obtained from a time derivative of the poloidal flux. Nevertheless, the results qualitatively demonstrate the off-axis contribution of LHCD to the current drive. Note that time points which were averaged to produce $J_{LH}(r)$ shown in Figure 6 were selected to encompass a quasi-stationary period of the Lower Hybrid heating phase that free of MHD activity, which started in that discharge at about t = 1.07 seconds. The evolution in loop voltage inferred from the intra-shot calibration technique follows the expected behavior as illustrated in Figure 7: at the start of LHCD the loop voltage changes first near the plasma edge, and then the change penetrates inward as time proceeds with a relaxation time of ∼200 ms.

V. CONCLUSIONS

The Motional Stark Effect diagnostic used on Alcator C-Mod experiences a significant, spurious drift in its measurement of magnetic pitch angle due to thermal-stress induced birefringence on a pair of in-vessel lenses. To circumvent this problem, an 'intra-shot' calibration technique has been developed that infers the current profile in the Ohmic phase prior to the start of LHCD from standard magnetic reconstructions (EFIT), constrained by measurements of the sawtooth inversion radius, and then uses MSE only to measure the change in pitch angle during LHCD. The intra-shot technique adequately reproduces the timing of disappearance and reappearance of sawteeth during LHCD and the measurements of kinetic stored energy.

Direct MSE pitch angle measurements during scans of $n_{||}$ at constant lower hybrid power, plasma density and plasma current clearly demonstrate larger changes in pitch angle as $n_{||}$ is reduced. The on-axis current density is observed to decrease from 20 to 12 MA/m^2 (at constant total $I_p = 0.8$ MA), at $P_{LH} = 0.9$ MW, $n_{||} = 1.56$, $\bar{n}_e = 6 \times 10^{19}$ m^{-3}, consistent with off-axis current drive by Lower Hybrid. The contribution of pure Ohmic induction to the total current density during LHCD has been estimated, which allows an inference of the current density profile $J_{LH}(r)$ that is driven by Lower Hybrid. It is observed that the plasmas evaluated in this study achieved off-axis Lower Hybrid current profiles with a broad maximum at $r/a = 0.3$.

ACKNOWLEDGMENTS

This work was supported by the U.S. Department of Energy under Contract Nos. DE-FC02-99ER54512 and DE-AC02-09CH11466.

[1] I. H. Hutchinson, R. Boivin, F. Bombarda, P. Bonoli, S. Fairfax, C. Fiore, J. Goetz, S. Golovato, R. Granetz, M. Greenwald, S. Horne, A. Hubbard, J. Irby, B. LaBombard, B. Lipschultz, E. Marmar, G. McCracken, M. Porkolab, J. Rice, J. Snipes, Y. Takase, J. Terry, S. Wolfe, C. Christensen, D. Garnier, M. Graf, T. Hsu, T. Luke, M. May, A. Niemczewski, G. Tinios, J. Schachter, and J. Urbahn, Phys. Plasmas **1**, 1511 (1994).

[2] F. M. Levinton, R. J. Fonck, G. M. Gammel, R. Kaita, H. W. Kugel, E. T. Powell, and D. W. Roberts, Phys. Rev. Lett. **63**, 2060 (1989).

[3] H. Y. Yuh, *The motional Stark effect diagnostic on Alcator C-Mod*, Ph.D. thesis, Massachusetts Institute of Technology (2005).

[4] D. I. Simon, N. L. Bretz, E. Marmar, R. Bravenec, and R. F. Parsells, in *Proc. 18th Symp. Fusion Engineering* (1999) p. 349.

[5] N. P. Basse, A. Dominguez, E. M. Edlund, C. L. Fiore, R. S. Granetz, A. E. Hubbard, J. W. Hughes, I. H. Hutchinson, J. H. irby, B. LaBombard, L. Lin, Y. Lin, B. Lipschultz, J. E. Liptac, E. S. Marmar, D. A. Mossessian, R. R. Parker, M. Porkolab, J. E. Rice, J. A. Snipes, V. Tang, J. L. Terry, S. M. Wolfe, S. J. Wukitch, K. Zhurovich, R. V. Bravenec, P. E. Phillips, W. L. Rowan, G. J. Kramer, G. Schilling, S. D. Scott, and S. J. Zweben, Fusion Sci. Technol. **51**, 476 (2007).

[6] J. Ko, S. Scott, M. Bitter, and S. Lerner, Rev. Sci. Instrum. **79**, 10F520 (2008).

[7] J. Ko, *Current profile measurements using MSE on Alcator C-Mod*, Ph.D. thesis, Massachusetts Institute of Technology (June 2009).

[8] J. Ko, S. Scott, S. Shiraiwa, R. Mumgaard, and M. Smith, in *Bull. Am. Phys. Soc.*, Vol. 54 (2009) p. 229.

[9] R. Mumgaard, S. Scott, J. Ko, S. Shiraiwa, and M. Smith, in *Bull. Am. Phys. Soc.*, Vol. 54 (2009) p. 229.

[10] P. T. Bonoli, J. Ko, R. Parker, A. E. Schmidt, G. Wallace, J. C. Wright, C. L. Fiore, A. E. Hubbard, J. Irby, E. Marmar, M. Porkolab, D. Terry, S. M. Wolfe, S. J. Wukitch, the Alcator C-Mod Team, J. R. Wilson, S. Scott, E. Valeo, C. K. Phillips, and R. W. Harvey, Phys. Plasmas **15**, 056117 (2008).

[11] J. R. Wilson, R. Parker, M. Bitter, P. T. Bonoli, C. Fiore, R. W. Harvey, K. Hill, A. E. Hubbard, J. W. Hughes, A. Ince-Cushman, C. Kessel, J. Ko, O. Meneghini, C. K. Phillips, M. Porkolab, J. Rice, A. E. Schmidt, S. Scott, S. Shiraiwa, E. Valeo, G. Wallace, J. C. Wright, and the Alcator C-Mod Team, Nucl. Fusion **49**, 115015 (2009).

[12] R. Parker, P. T. Bonoli, O. Meneghini, M. Porkolab, A. E. Schmidt, S. Shiraiwa, G. Wallace, J. R. Wilson, A. E. Hubbard, J. W. Hughes, J. Ko, R. M. McDermott, M. L. Reinke, J. E. Rice, and S. Scott, in *18th Topical Conference on RF Power in Plasmas* (2009).

[13] L. L. Lao, H. S. John, R. D. Stambaugh, and W. Pfeiffer, Nucl. Fusion **25**, 1421 (1985).

[14] L. L. Lao, H. S. John, R. D. Stambaugh, A. G. Kellman, and W. Pfeiffer, Nucl. Fusion **25**, 1611 (1985).

[15] L. L. Lao, J. R. Ferron, R. J. Groebner, W. Howl, H. S. John, E. J. Strait, and T. S. Taylor, Nucl. Fusion **30**, 1035 (1990).

[16] P. Phillips, A. Lynn, K. Gentle, W. Rowan, A. Hubbard, M. Greenwald, and D. Mikkelson, in *Bull. Am. Phys. Soc.*, Vol. 47 (2002).

[17] J. Wesson, *Tokamaks*, 2nd ed. (Clarendon Press, Oxford, 1997).

The Princeton Plasma Physics Laboratory is operated
by Princeton University under contract
with the U.S. Department of Energy.

Information Services
Princeton Plasma Physics Laboratory
P.O. Box 451
Princeton, NJ 08543

Phone: 609-243-2245
Fax: 609-243-2751
e-mail: pppl_info@pppl.gov
Internet Address: http://www.pppl.gov